

a_i^K refer to a particular state $\{a_i^K\}$, the superscript K will often be omitted.

²⁴F. B. Hildebrand, *Methods of Applied Mathematics* (Prentice-Hall, Englewood Cliffs, N. J., 1952).

²⁵In order to calculate numerically the quantities F_i and B_{ij} , a specific model for interatomic interactions is of course required. The means of evaluating these quantities for the case of central two-body interactions between atoms will be discussed in Sec. II C.

²⁶D. H. Tsai and C. W. Beckett, *J. Geophys. Res.* **71**, 2601 (1966).

²⁷L. A. Girifalco and V. G. Weizer, *J. Phys. Chem. Solids* **12**, 260 (1960).

²⁸The compressibility β of a cubic crystal is equal to $\frac{1}{3}(C_{11} + 2C_{12})$, where C_{11} and C_{12} are the elastic constants.

From the definitions of the elastic constants in terms of energy density, it follows that $C_{11} = B_{11}^0/a^0$ and $C_{12} = B_{12}^0/a^0$; thus $\beta = (1/3a^0)(B_{11}^0 + 2B_{12}^0)$, where B_{11}^0 and B_{12}^0 are given by Eqs. (53) and (54) for lattice parameters $a_i = a_i^0$ [the second summation in Eq. (53) is identically zero since $F_1 = 0$ for $a_i = a_i^0$].

²⁹The lattice is referred to as "bcc lattice" or as a "stressed bcc lattice" even though $a_2 = a_3 \neq a_1$ for $a_1 \neq a^0$.

³⁰A. H. Cottrell, *Theoretical Structural Metallurgy*, 2nd ed. (Edward Arnold and Co., London, 1955), p. 135.

³¹J. C. Crump III and J. W. Mitchell, *J. Appl. Phys.* **41**, 717 (1970).

³²S. S. Brenner, *J. Appl. Phys.* **27**, 1484 (1956).

³³S. S. Brenner, *Science* **128**, 569 (1958).

Debye-Waller Factors of Cubic Metals

Narain Singh and P. K. Sharma

Physics Department, University of Allahabad, Allahabad, India

(Received 16 June 1970)

The exponents of the Debye-Waller factor for the cubic metals copper, silver, gold, aluminium, nickel, sodium, chromium, and α -iron are determined at different temperatures from the vibrational spectrum derived from a model for the lattice dynamics of metals recently propounded by Chéveau, which includes the influence of conduction electrons on lattice vibrations. The calculation uses Blackman's root-sampling technique for a discrete subdivision in wave-vector space. The results of the calculations are compared with available experimental data in terms of the Debye-Waller-factor temperature parameter Y , the effective x-ray characteristic temperature Θ_M , and the mean-square displacement of the atoms \bar{u}^2 . Except for chromium, the theoretical values show reasonably satisfactory agreement with the experimental measurements.

I. INTRODUCTION

In the nonresonant elastic scattering of waves (slow neutrons, x rays, etc.) from scatterers which are bound in crystals, the fall in the intensity on account of lattice thermal motion is governed by an exponential factor e^{-2M} , called the Debye-Waller factor. The exponent $2M$ depends upon the mean-square displacement of the atoms, and can be correlated with many other solid-state phenomena. In the recent past, considerable interest has been shown in the experimental study of the thermal variation of the Debye-Waller factors of metals by means of x-ray diffraction. The experimental data have usually been interpreted in terms of the Debye theory, using volume-change corrections due to Paskin.¹

It is now well known that electrons in metals influence considerably the vibrational frequencies and their lattice-dynamical behavior. In recent years, a number of models²⁻⁴ have been propounded for calculating the phonon frequencies of metals by taking cognizance of electrons in various approximate ways. However, many of these models violate

some symmetry properties of a cubic lattice. Lax⁵ has attributed this inadequacy to the neglect of translational invariance of the lattice. Recently, Krebs⁶ has attempted to remove this difficulty by considering umklapp processes. However, this model suffers from a serious defect of internal equilibrium, i.e., the derivative of the long-range screened Coulomb interaction energy does not vanish at the equilibrium configuration as it does for the short-range Born-von Kármán term. This necessitates external forces to maintain the system in equilibrium. Quite recently, Chéveau⁷ has propounded a model for the dispersion of lattice waves in cubic metals which satisfies the symmetry requirements of a cubic lattice and preserves internal equilibrium without recourse to any external force. The model considers the ion-ion interaction as the first two terms in Taylor expansion of the potential energy. For the electron-ion interaction, the linearized Thomas-Fermi equation is used over the whole crystal. The model has recently been used by the authors⁸ to study the thermal variations of the Grüneisen parameters of cubic metals and was found to give

satisfactory agreement with experimental values. It would be interesting to use this model for other solid phenomena to provide a further check on the accuracy of the model.

In this paper, we present a calculation of the temperature variation of the Debye-Waller-factor exponents and the mean-square displacements of the atoms in cubic metals copper, silver, gold, aluminium, nickel, sodium, chromium and α -iron on the basis of the Chéveau model. The choice of these metals for this study was dictated by the fact that several authors have extensively investigated the elastic properties of these metals, and thermal variations of the effective characteristic temperature from x-ray intensity measurements are available for them over a wide temperature range.

II. THEORY

In the quasiharmonic approximation, the exponent of the Debye-Waller factor is related to the mean-square displacement of the atoms and is given by⁹

$$2M = \langle |\vec{K} \cdot \vec{u}(n)|^2 \rangle, \quad (1)$$

where $\vec{u}(n)$ is the displacement of the n th atom and \vec{K} is the difference of the initial and the final wave vectors of the wave. Using the standard theory, Eq. (1) can be written in terms of eigenvalues and eigenvectors of the vibrational spectrum in the form

$$2M = \frac{\hbar}{mN} \sum_{\vec{q}, p} \frac{(\vec{K} \cdot \vec{e}_{\vec{q}, p})^2}{\omega_{\vec{q}, p}} \left(\frac{1}{2} + \frac{1}{\exp(\hbar \omega_{\vec{q}, p} / kT) - 1} \right), \quad (2)$$

where m is the mass of an atom in the lattice, N is the total number of unit cells in the crystal, $\omega_{\vec{q}, p}$ is the angular frequency of a phonon of wave vector \vec{q} and polarization p , $\vec{e}_{\vec{q}, p}$ is the polarization vector of the \vec{q}, p lattice mode, \hbar is Planck's constant divided by 2π , k is Boltzmann's constant, and T is the absolute temperature, and the summation extends over all the normal vibrations of the crystal. In the case of cubic crystals, using symmetry considerations, the polarization factor $(\vec{K} \cdot \vec{e}_{\vec{q}, p})^2$ can be replaced by its average value outside the summations. If $G(\omega)$ is the frequency-distribution function for the phonon giving the number of vibrational modes in the frequency interval ω and $\omega + d\omega$, Eq. (2) becomes

$$2M = \frac{8\pi^2 \hbar}{3mN} \left(\frac{\sin \theta}{\lambda} \right)^2 \int_0^{\omega_m} \frac{\omega G(\omega)}{\omega} \coth \frac{\hbar \omega}{2kT} d\omega, \quad (3)$$

where ω_m is the maximum frequency of the vibration spectrum, θ is the Bragg angle, and λ is the wavelength of the incident radiation. From Eq. (1), the mean square of total displacements of an atom from the average position is given by

$$\overline{u^2} = 3\lambda^2 \overline{M} / 8\pi^2 \sin^2 \theta. \quad (4)$$

For a Debye model of the solid, denoting the characteristic temperature by Θ_M , the temperature dependence of the Debye-Waller-factor exponent can be written as

$$2M = \frac{48\pi^2 \hbar^2}{mk\Theta_M} \left(\frac{\Phi(x)}{x} + \frac{1}{4} \right) \left(\frac{\sin \theta}{\lambda} \right)^2, \quad (5)$$

where $\Phi(x)$ is the usual Debye integral function, and $x = \Theta_M/T$.

If $G(\omega)$ is known, Eq. (3) can be used to calculate $2M$ and hence $\overline{u^2}$ and Θ_M from Eqs. (4) and (5). In the present work we have used the Chéveau⁷ model for the evaluation of $G(\omega)$.

III. NUMERICAL COMPUTATION

The calculation of the Debye-Waller-factor exponent $2M$ from Eq. (3) at different temperatures has been made by Blackman's root-sampling technique¹⁰ for a discrete subdivision in wave-vector space. To have a fairly large survey of frequencies, we have considered a mesh of evenly spaced 8000 wave vectors in the first Brillouin zone. For this purpose, the first Brillouin zone was divided into $20 \times 20 \times 20$ miniature cells with axes $\frac{1}{20}$ of the length of the reciprocal-lattice cell. Using the symmetry considerations, the vibrational frequencies were determined from the roots of the Chéveau⁷ secular determinant at nonequivalent points in the irreducible $\frac{1}{48}$ part of the first Brillouin zone. Each frequency was weighted according to the symmetrically equivalent points. The number of frequencies lying in each of the intervals 0.1×10^{13} rad/sec were counted, and a histogram of the vibrational spectrum was obtained. Using this histogram, the Debye-Waller-factor exponent $2M$ was evaluated by numerical integration of Eq. (3). In the calculation, the screening parameter of the electron-ion interaction was considered as an adjustable parameter, the best-fit values of which were obtained from the experimental dispersion curves. The mean-square displacements of atoms $\overline{u^2}$ at different temperatures were evaluated from Eq. (4) and the corresponding effective characteristic temperature Θ_M is obtained from Eq. (5). The numerical values of the elastic constants and other relevant parameters for the metals used in the calculations are collected in Table I.

IV. COMPARISON WITH EXPERIMENTS

The comparison between theory and experimental data on x-ray intensity measurements is made in terms of the Debye-Waller-factor temperature parameter Y given by

$$Y = (2 \log_{10} e) (\lambda / \sin \theta)^2 (M_0 - M_T), \quad (6)$$

where M_0 and M_T are the values of M at temperatures T_0 and T , respectively. This quantity is in-

TABLE I. Lattice constant and elastic constants for cubic metals used in the calculation.

Metal	Lattice constant Å	Elastic constants (10^{11} dyn/cm ²)			Reference
		C ₁₁	C ₁₂	C ₄₄	
Copper	3.616	16.839	12.142	7.539	a
Silver	4.080	12.399	9.367	4.612	b
Gold	4.070	19.234	16.314	4.195	b
Aluminum	4.050	10.678	6.074	2.821	c
Nickel	3.524	25.280	15.200	12.380	d
Sodium	4.291	0.741	0.624	0.419	e
Chromium	2.880	35.000	6.780	10.080	f
α -Iron	2.866	23.310	13.544	11.783	g

^aW. C. Overton and J. Gaffney, Phys. Rev. 98, 969 (1955).

^bJ. R. Neighbours and G. A. Alers, Phys. Rev. 111, 707 (1958).

^cG. N. Kamm and G. Alers, J. Appl. Phys. 35, 327 (1964).

^dJ. R. Neighbours, F. W. Bratten, and C. S. Smith, J. Appl. Phys. 23, 389 (1952).

^eW. B. Daniels, Phys. Rev. 119, 1246 (1960).

^fD. I. Bolef and J. de Klerk, Phys. Rev. 129, 1063 (1963).

^gJ. A. Rayne and B. S. Chandrasekhar, Phys. Rev. 122, 1714 (1961).

dependent of λ and θ , and is solely dependent upon the vibrational spectrum. The values of Y are directly accessible from the measured intensities of the Bragg reflection in x-ray diffraction experiments. If R_T and R_0 are measured integrated intensities of a certain diffraction line at temperatures T and T_0 , respectively, we have

$$Y = (\lambda/\sin\theta)^2 \log_{10} (R_T/R_0). \quad (7)$$

The calculated values of Y and $\overline{u^2}$ from Eqs. (3), (4), and (6) at different temperatures for copper, silver, gold, aluminium, nickel, sodium, chromium, and α -iron are presented in Figs. 1–8, respectively. In these figures, we have also shown the effective Debye temperature Θ_M obtained from Eq. (5) for the calculated Debye-Waller-factor exponents. For comparison, the values of Y , $\overline{u^2}$, and Θ_M deduced from experimental x-ray intensity measurements have also been plotted in these figures.

A. Copper

The temperature variation of the Debye-Waller factor of copper from x-ray intensity measurements has been studied by Flinn *et al.*,¹¹ Owen and Williams,¹² and Chipman and Paskin.¹³ Flinn *et al.*¹¹ have measured the integrated intensities of the (600), (800), and (1000) reflections from a single copper crystal at selected temperatures in the temperature range 4.2–500 °K. These authors have expressed their results in terms of the effective Debye temperature Θ_M . Owen and William's¹² measurements covered the range from room temperature (293 °K) to 900 °K for microphotometric measurements on the lines in x-ray structure spectra of powder specimens. They have tabulated the values of Y at selected temperatures. Both these measurements are

consistent and agree with those of Chipman and Paskin¹³ at room and liquid-nitrogen temperatures on copper powder. The values of Y , $\overline{u^2}$, and Θ_M deduced from the experimental data of these workers are plotted in Fig. 1. The reference temperature T_0 is taken as 293 °K. The agreement of the calculated values with experiments is reasonably satisfactory.

B. Silver

The temperature dependence of the Debye characteristic temperature of silver from relative intensity measurements of Bragg reflections has been determined by several authors^{14–18} by using slightly different techniques. Boskovits *et al.*¹⁴ measured the integrated intensities of diffraction lines (111) and (422) from a silver wire at six different temperatures between 81 and 774 °K. To eliminate errors due to the fluctuations of the primary intensities and the efficiency of the counter, they measured the ratio of intensity of two lines in a number of runs. Their results show rapid decrease of Θ_M with increasing temperature beyond 290 °K, which do not coincide with those of other workers. Andriessen¹⁵ used silver powder and carried out intensity measurements over several diffraction lines. Though he worked from room temperature (291 °K) to 875 °K, he has tabulated his results for the temperature region 607 to 875 °K. His measurements are, however, not sufficiently accurate, since they were affected by the change in extinction effects and by the oxidation of the surface of the scattering material. Spreadborough and Christian¹⁶ have measured the peak intensities of diffracted powder lines (511)/(333), (422), and (420) in the temperature range 273–1343 °K. Their effective Θ_M values are about

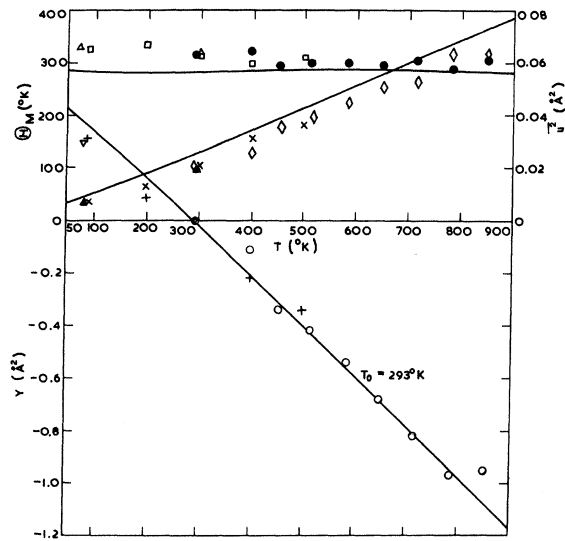


FIG. 1. Temperature dependence Y , $\overline{u^2}$, and Θ_M for copper. Full lines show the present calculations. Experimental points: ∇ , \times , \square , Flinn *et al.*; \circ , \diamond , \bullet , Owen and Williams; \blacktriangle , \triangle , Chipman and Paskin.

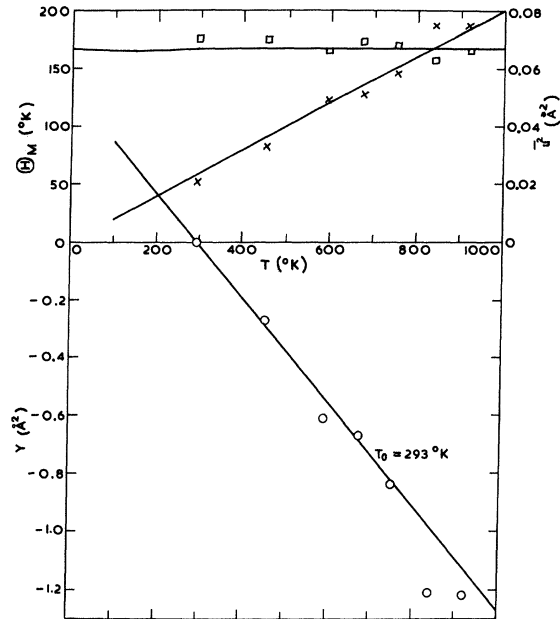


FIG. 3. Variation of γ , $\overline{u^2}$, and Θ_M for gold. Full lines depict the present calculations. Experimental points: \circ , \times , \square , Owen and Williams.

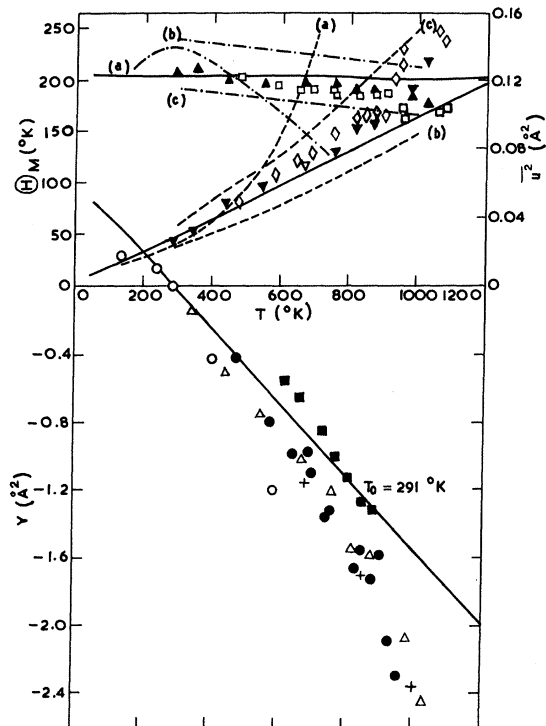


FIG. 2. Temperature variation of Y , $\overline{u^2}$, and Θ_M for silver. Full lines show the present calculations. Experimental measurements: \circ , (a) Boskovits *et al.*; \blacksquare , (b) Andriessen; $+$, (c) Spreadborough and Christian; \bullet , \diamond , \square , Haworth; ∇ , \blacktriangledown , \blacktriangle , Simerská.

22% lower than those obtained by Andriessen. Haworth's¹⁷ measurements can be considered to be most exhaustive and reliable. He has measured integrated as well as peak intensities of diffraction lines (331), (511)/(333), and (422) for a silver-powder specimen in the temperature range 286–1100 °K, taking account of the thermal contribution to Bragg's peak and repeatedly annealing the specimen at 1220 °K. His values are in excellent agreement with the measurements of Simerská,¹⁸ who has covered the temperature range 291–1033 °K for several diffraction lines using a bent crystal of Johansson type, but differ considerably from those of Boskovits *et al.*,¹⁴ Andriessen,¹⁵ and Spreadborough and Christian.¹⁶ For comparison, the values of Y , $\overline{u^2}$, and Θ_M deduced from measured intensities of all these workers are plotted in Fig. 2. The agreement between the theoretical and experimental values of Y is satisfactory up to about 900 °K. At higher temperatures, the observed diminution in the intensity is greater than expected theoretically and the discrepancy increases with the rise of temperature. The theoretical results for $\overline{u^2}$ and Θ_M show reasonably satisfactory agreement with measurements by Haworth¹⁷ and Simerská.¹⁸

C. Gold

The thermal variation of the Debye-Waller factor for gold has been studied by Owen and Williams¹² by making measurements of the integrated intensities of x-ray Bragg reflections at temperatures ranging

from room temperature (293 °K) to 900 °K. As in the case of copper, their investigations have been both thorough and extensive. They have tabulated the values of Y at selected temperatures. These are plotted in Fig. 3 with $T_0 = 293$ °K along with the values of $\overline{u^2}$ and Θ_M deduced from their intensity measurements. The theoretical results agree satisfactorily with experimental values.

D. Aluminium

Measurements of the temperature variations of the integrated intensities of x-ray reflections from aluminium have been made by Backhurst,¹⁹ Collins,²⁰ James *et al.*,²¹ Owen and Williams,¹² Chipman,²² and Flinn and McManus.²³ The first two measurements are not very accurate, being affected by the recrystallization and annealing effects due to heating, and differ appreciably from those of other workers. The first reliable measurements of the integrated intensities of x-ray reflections from a single aluminium crystal are those of James *et al.*²¹ at liquid air and room temperature (290 °K). Owen and Williams¹² made extensive microphotometric measurements of x-ray reflections from a powder specimen in the temperature range 293–900 °K and tabulated the values of Y for selected temperatures. Their data show considerable scatter beyond 600 °K, but there is reasonable agreement among the experimentally determined slopes. Chipman²² measured the integrated intensities of the high-angle x-ray diffraction peaks in the temperature range 60–880 °K and corrected them for the thermal diffuse scattering. His measured temperature dependence agrees well with those of Owen and Williams¹² and other workers. Flinn and McManus²³ measured x-ray Debye Θ_M of aluminium in the temperature range 4.2–400 °K using a flat single crystal with faces cut parallel to (100) planes. They have also worked out the Debye-Waller factor of aluminium using a model of the solid with nearest-neighbor central and noncentral interactions. For the present comparison, we have chosen the data of James *et al.*,²¹ Owen and Williams,¹² Chipman,²² and Flinn and McManus.²³ These are plotted in Fig. 4 with $T_0 = 293$ °K. The agreement of the calculated Y values with experiments is reasonably satisfactory. Below 700 °K, the calculated $\overline{u^2}$ values are slightly higher than those obtained from the observed fall in intensity, while the calculated Θ_M lies below the observed ones.

E. Nickel

Experimental study of temperature variation of the x-ray Debye characteristic temperature of nickel has been reported by Simerská²⁴ and Wilson *et al.*²⁵ Simerská has taken observations from 293–873 °K using a flat polycrystalline sample of nickel. Wilson *et al.*, on the other hand, have measured integrated intensities for a single crystal in the

temperature range 100–520 °K and have corrected the data for thermal diffuse scattering and change of lattice parameter. The two measurements compare favorably throughout the range of their measurements. These are plotted in Fig. 5 with $T_0 = 298$ °K. A reasonably satisfactory agreement is found between the theoretical and experimental values of Y . However, the experimental Θ_M are consistently higher than the theoretical values, while the experimental $\overline{u^2}$ values are lower than the theoretical values.

F. Sodium

Dawton²⁶ has studied the thermal variation of the Debye characteristic temperature of sodium by making x-ray intensity measurements from a single crystal in the temperature range 117–368 °K. He has measured the intensity ratios R_{117}/R_T for the chilled crystal for (110), (200), (220), (310), (400), and (440) reflections at three different temperatures. Of these only (220), (310), and (400) reflections are reliable. The average values of Y , $\overline{u^2}$, and Θ_M obtained from these three reflections are plotted in Fig. 6. The agreement is reasonably satisfactory, though observed Θ_M values somewhat exceed the calculated curve.

G. Chromium

The temperature variation of the Debye temper-

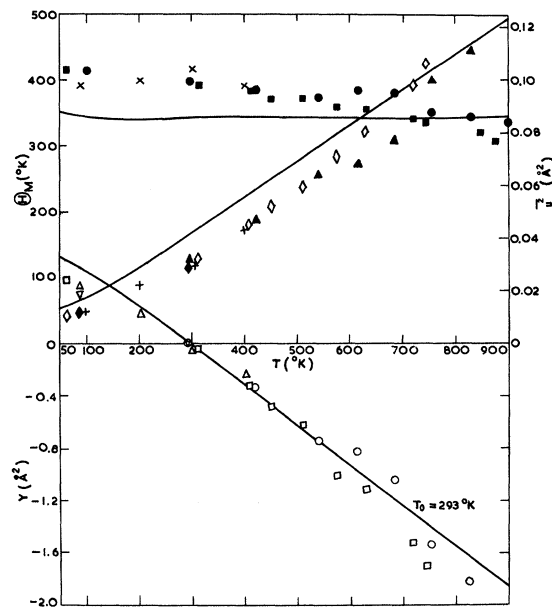


FIG. 4. Temperature dependence of Y , $\overline{u^2}$, and Θ_M for aluminium. Solid curves are based on present calculations. Experiment points: ∇ , \blacklozenge , James *et al.*; \circ , \triangle , \bullet , Owen and Williams; \square , \diamond , \blacksquare , Chipman; \triangle , $+$, \times , Flinn and McManus.

ature of chromium from relative intensity measurements of x-ray reflections by a single crystal has been studied by Wilson *et al.*²⁵ in the temperature range 100–520 °K. They have corrected the data for thermal diffuse scattering and change in lattice parameter. Ilyina and Kristskaya²⁷ have also reported the measurement of x-ray Debye temperature of chromium, but their measurements are confined to room temperature only. The experimental values of Wilson *et al.*²⁵ are compared with the present calculations in Fig. 7. There is reasonably satisfactory agreement between the theoretical and experimental Y values, but u^2-T and Θ_M-T curves show large deviations in the theoretically and experimentally determined values. For example, the calculated Θ_M are lower than experimental values by 25% at 100 °K and by 18% at 500 °K. The marked discrepancy may partly be attributed to uncertainty in the determination of integrated intensities. It appears that some other factor predominates in the case of chromium.

H. α -Iron

Measurements of the Debye-Waller factor of α -iron have been made both through x-ray diffraction^{17,27,28} and γ -ray resonant absorption²⁹ experiments. The x-ray measurements of Haworth¹⁷ covered the temperature range 286–1190 °K by

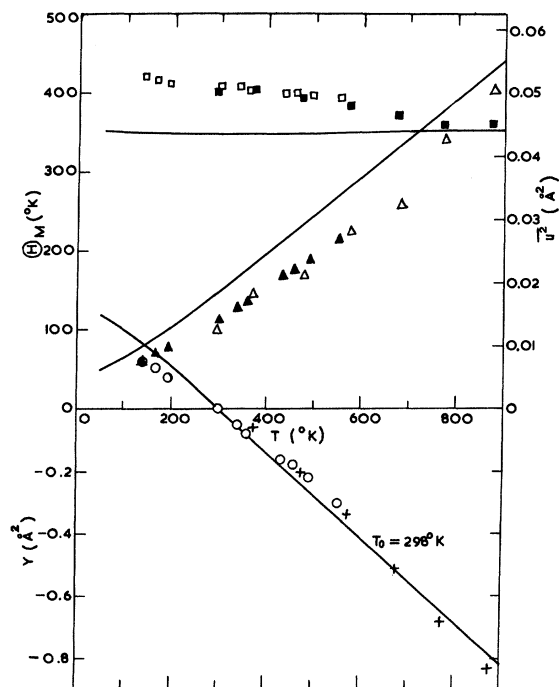


FIG. 5. Variation of Y , u^2 , and Θ_M for nickel. Solid lines show the present calculations. Experimental points: +, Δ , \blacksquare , Simerská; \circ , \blacktriangle , \square , Wilson *et al.*

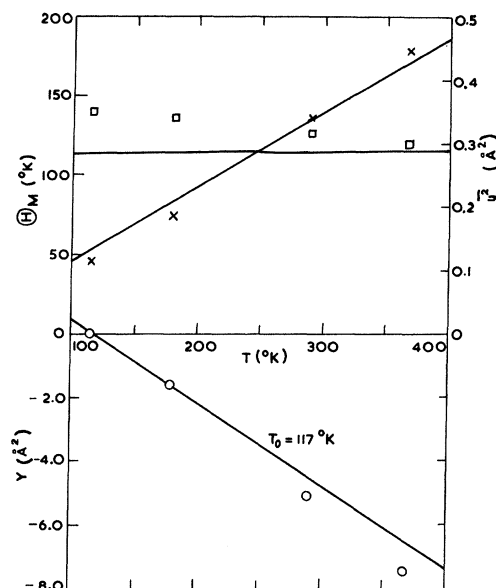


FIG. 6. Variation of Y , u^2 , and Θ_M with temperature for sodium. Solid curves show the present calculations. Experimental points: \circ , X, \square , Dawton.

making integrated intensities and peak-height measurements of the diffraction line (220) for an iron specimen. The results show large scatter associated with crystal changes brought about by prolonged

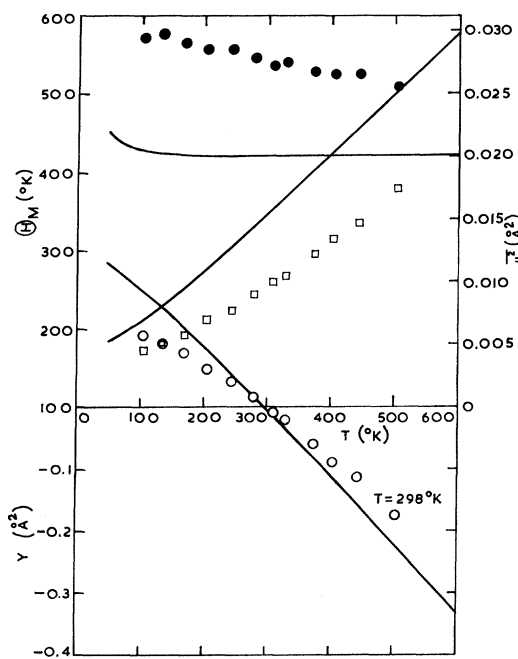


FIG. 7. Temperature dependence of Y , u^2 , and Θ_M for chromium. Continuous curves show the present calculations. Experimental points: \circ , \square , \bullet , Wilson *et al.*

TABLE II. Comparison of the calculated x-ray Θ_M° and experimental calorimetric Θ_C° at 0 °K for cubic metals.

Metal	x-ray Θ_M° (°K) (Present work)	Calorimetric Θ_C° (°K) (Experimental)
Copper	285	345.8 ^a
Silver	204	227.3 ^a
Gold	168	162.3 ^a
Aluminium	364	427.7 ^b
Nickel	356	440 ^c
Sodium	114	156.6 ^d
Chromium	508	630 ^e
α -Iron	384	470 ^e

^aD. L. Martin, Phys. Rev. **170**, 650 (1968).

^bN. E. Phillips, Phys. Rev. **114**, 676 (1959).

^cJ. A. Rayne and W. R. G. Kemp, Phil. Mag. **1**, 918 (1956).

^dD. L. Martin, Phys. Rev. **124**, 438 (1961).

^eG. Duyckaerts, Physica **6**, 401 (1939).

annealing. The x-ray intensity measurements for iron by Ilyina and Kristkaya,²⁷ and by Herbstein and Smuts²⁸ refer to room temperature only and are therefore not chosen for the present comparison. The experimental data of Haworth¹⁷ are plotted in Fig. 8 along with a few experimental measurements of Debrunner and Morrison²⁹ in the temperature range 293–573 °K. The theoretical results agree reasonably well with experiments, though the x-ray measurements show large scatter.

It would be interesting to evaluate the x-ray Debye temperature for $T=0$ °K and compare it with those deduced from low-temperature specific-heat measurements. Table II gives the limiting values of Θ_M obtained from the present theory together with the values deduced from low-temperature specific-heat data. It will be seen that the two values show reasonably satisfactory agreement. As expected, the x-ray values are, in general, found to be somewhat lower than the calorimetric Debye temperature obtained from observed specific-heat measurements, owing to different averaging over the vibrational mode.³⁰ If the vibrational spectrum has the Debye form, the x-ray Θ_M should be equal to the calorimetric Θ_C . In general, the effect of the actual vibrational spectrum is to lower the x-ray value in comparison with the specific-heat values.

V. DISCUSSION

A study of Figs. 1–8 shows that the Debye-Waller-factor temperature parameter Y obtained from the Chéveau model provides a reasonable description of observed temperature variation of the intensities of x-ray reflections up to a certain temperature. In the higher temperature regions, the observed

Y -vs- T curves show marked nonlinearity; the observed fall in the intensity becomes greater than the theoretical decrease and the divergence between them increases with temperature. The effective x-ray characteristic temperature obtained here appears to show similar behavior with experiments although there are large uncertainties in the experimental values of Θ_M . The disagreement is, however, more pronounced in the case of chromium. The theoretical mean-square displacements of the atoms lie somewhat above the experimental measurements, the maximum discrepancy occurring in the case of chromium.

The apparent discrepancy between theory and experiment is not unexpected, and can be attributed to the neglect of the temperature variation of the vibrational frequencies¹ and to other anharmonic effects.^{31–33} In the present work, no account has been taken of the temperature variation of the elastic constants and the lattice parameter. With the increase of temperature, lattice frequencies are diminished because of lattice expansion. This effect depends upon the Grüneisen parameter which varies with temperature and lattice frequencies. Several attempts^{12,16,17} have been made to account for this effect in terms of the Grüneisen parameter. However, the available data do not allow a detailed discussion. It appears that there is a need of more detailed studies to relate this parameter with anharmonicity in lattice vibrations in order to obtain bet-

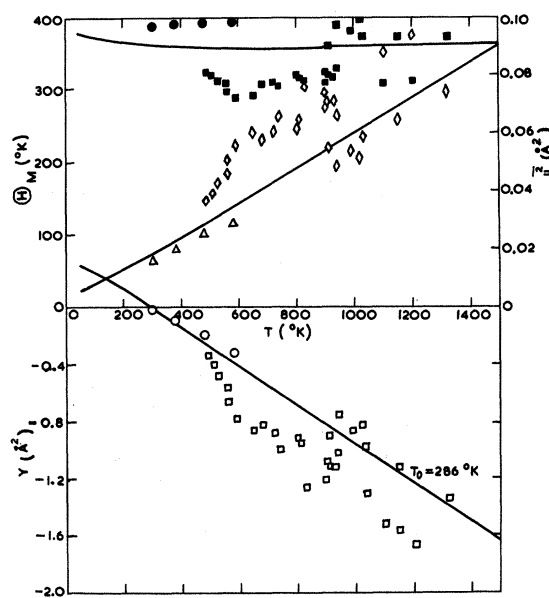


FIG. 8. Variation of Y , u^2 , and Θ_M for α -iron. Solid curves depict the present calculations. Experimental points: \square , \diamond , \blacksquare , Haworth; \circ , \triangle , \bullet , Debrunner and Morrison.

ter agreement between theory and experiment. At the present level of accuracy, the present agreement indicates that the Chéveau model is adequate for the interpretation of x-ray Debye-Waller-factor data of cubic metals.

ACKNOWLEDGMENTS

The authors are thankful to the Council of Scientific and Industrial Research, New Delhi, for financial support, and to Professor Vachaspati for encouragement.

- ¹A. Paskin, *Acta Cryst.* **10**, 667 (1957).
²J. de Launay, *J. Chem. Phys.* **21**, 1975 (1953); in *Solid State Physics*, edited by F. Seitz and D. Turnbull (Academic, New York, 1956), Vol. 2, p. 220.
³A. B. Bhatia, *Phys. Rev.* **97**, 363 (1955); A. B. Bhatia and G. K. Horton, *ibid.* **98**, 1715 (1955).
⁴P. K. Sharma and S. K. Joshi, *J. Chem. Phys.* **39**, 2633 (1963); **40**, 662 (1964).
⁵M. Lax, in *Proceedings of the International Conference on Lattice Dynamics, Copenhagen*, 1963, edited by R. F. Wallis (Pergamon, New York, 1964), p. 179.
⁶K. Krebs, *Phys. Rev.* **138**, A143 (1965).
⁷L. Chéveau, *Phys. Rev.* **169**, 496 (1968).
⁸P. K. Sharma and N. Singh, *Phys. Rev. B* **1**, 4635 (1970).
⁹R. W. James, *The Optical Principles of the Diffraction of X-rays* (G. Bell and Sons, London, 1954), p. 193.
¹⁰M. Blackman, in *Handbuch der Physik*, edited by S. Flügge (Springer, Berlin, 1955), Vol. 7, p. 325.
¹¹P. A. Flinn, G. M. McManus, and J. A. Rayne, *Phys. Rev.* **123**, 809 (1961).
¹²E. A. Owen and R. W. Williams, *Proc. Roy. Soc. (London)* **A188**, 509 (1947).
¹³D. R. Chipman and A. Paskin, *J. Appl. Phys.* **30**, 1992 (1959).
¹⁴J. Boskovits, M. Roilos, A. Theodossiou, and K. Alexopoulos, *Acta Cryst.* **11**, 845 (1958).
¹⁵R. Andriessen, *Physica* **2**, 417 (1935).
¹⁶J. Spreadborough and J. W. Christian, *Proc. Phys. Soc. (London)* **74**, 609 (1959).
¹⁷C. W. Haworth, *Phil. Mag.* **5**, 1229 (1960).
¹⁸M. Simerská, *Acta Cryst.* **14**, 1259 (1961).
¹⁹I. Backhurst, *Proc. Roy. Soc. (London)* **A102**, 340 (1922).
²⁰E. H. Collins, *Phys. Rev.* **24**, 152 (1926).
²¹R. W. James, G. W. Brindley, and R. G. Wood, *Proc. Roy. Soc. (London)* **A125**, 401 (1929).
²²D. R. Chipman, *J. Appl. Phys.* **31**, 2012 (1960).
²³P. A. Flinn and G. M. McManus, *Phys. Rev.* **132**, 2458 (1963).
²⁴M. Simerská, *Czech. J. Phys.* **B12**, 858 (1962).
²⁵R. H. Wilson, E. F. Skelton, and J. L. Katz, *Acta Cryst.* **21**, 635 (1966).
²⁶R. H. V. M. Dawton, *Proc. Phys. Soc. (London)* **49**, 294 (1937).
²⁷V. A. Ilyina and V. K. Kristasya, in *Problems of Metallography and Physics of Metals, IV Symposium, Moscow*, 1955, edited by B. Ya Lyubov (English translation: U.S. Atomic Energy Commission Report No. 2924, U.S. GPO, Washington, D.C., 1956).
²⁸F. H. Herbstein and J. Smuts, *Phil. Mag.* **8**, 367 (1963).
²⁹P. Debrunner and R. J. Morrison, *Rev. Mod. Phys.* **36**, 463 (1964) [as quoted in J. Baijal, *Phys. Letters* **13**, 32 (1964)].
³⁰W. Cochran, *Rept. Progr. Phys.* **26**, 1 (1963).
³¹H. Hahn and W. Ludwig, *Z. Physik* **161**, 404 (1961).
³²A. A. Maradudin and P. A. Flinn, *Phys. Rev.* **129**, 2529 (1963).
³³R. A. Cowley, *Advan. Phys.* **12**, 421 (1963).

Graphite Carrier Locations and Quantum Transport to 10 T (100 kG)

John A. Woollam

National Aeronautics and Space Administration, Cleveland, Ohio 44135

(Received 12 June 1970)

The magnetoresistance, Hall effect, thermopower, thermal resistivity, and Nernst-Ettingshausen effects are measured in magnetic fields to 10.3 T (103 kG) and at temperatures between 1.1 and 4.2 K. Samples are highly ordered pressure-annealed pyrolytic graphite. The major results are that majority-carrier electrons and holes are assigned to specific locations in the Brillouin zone; the electrons are assigned to be around the center of the zone edge (point *K*). The first observation of spin-split Landau levels is made. A study of distorted line shapes of thermopower quantum oscillations shows agreement with a theory by Horton. Sugihara and Ono's theory, predicting field values for Landau level crossings of the Fermi energy in graphite, is confirmed for fields below 4 T.

I. INTRODUCTION

Pressure-annealed pyrolytic graphite is a highly ordered form of carbon,¹ but is not a single crystal. The lattice for a single crystal is hexagonal. For

pyrolytic samples there are individual crystallites with [0001] axes nearly parallel to each other, but [1100] axes, for example, are randomly oriented with respect to each other. Typical crystallite sizes are between 10 and 100 μ in diam. Because